

Northumbria Research Link

Citation: Kanesan, Thavamaran, Ng, Wai Pang, Ghassemlooy, Zabih and Lu, Chao (2014) Investigation of Optical Modulators in Optimized Nonlinear Compensated LTE RoF System. Journal of Lightwave Technology, 32 (10). pp. 1944-1950. ISSN 0733-8724

Published by: IEEE

URL: <http://dx.doi.org/10.1109/jlt.2014.2312321>
<<http://dx.doi.org/10.1109/jlt.2014.2312321>>

This version was downloaded from Northumbria Research Link:
<http://nrl.northumbria.ac.uk/id/eprint/23891/>

Northumbria University has developed Northumbria Research Link (NRL) to enable users to access the University's research output. Copyright © and moral rights for items on NRL are retained by the individual author(s) and/or other copyright owners. Single copies of full items can be reproduced, displayed or performed, and given to third parties in any format or medium for personal research or study, educational, or not-for-profit purposes without prior permission or charge, provided the authors, title and full bibliographic details are given, as well as a hyperlink and/or URL to the original metadata page. The content must not be changed in any way. Full items must not be sold commercially in any format or medium without formal permission of the copyright holder. The full policy is available online: <http://nrl.northumbria.ac.uk/policies.html>

This document may differ from the final, published version of the research and has been made available online in accordance with publisher policies. To read and/or cite from the published version of the research, please visit the publisher's website (a subscription may be required.)

Investigation of Optical Modulators in Optimized Nonlinear Compensated LTE RoF System

Thavamaran Kanesan, *Member, IEEE*, Wai Pang Ng, *Senior Member, IEEE*, Zabih Ghassemlooy, *Senior Member, IEEE*, and Chao Lu, *Member, IEEE*

Abstract— In this paper, we investigate a nonlinear compensation technique with two different architectures using direct modulation (DM) and external modulation (EM) techniques, termed as DM based frequency dithering (DMFD) and EM based frequency dithering (EMFD). We show that DMFD and EMFD methods operate substantially different in radio-over-fiber (RoF) system by optimizing the dithering technique relative to the LTE technology. The proposed techniques is only applicable if the condition of $\{f_L < f_d < f_{RF}\}$ is met, where f_L represents the dithering boundary limit of 14 MHz, f_d is DMFD signal frequency and f_{RF} is the RoF carrier frequency. Analysis of the optical launch power for DMFD and EMFD methods reveal that the stimulated Brillouin scattering (SBS) threshold is above ~ 6 dBm for the LTE-RoF system. In addition, we also unveil that DMFD and EMFD methods do not introduce additional distortion for the linear and optimum optical launch power regions, which are frequency chirp driven regions. If the given condition is met, the proposed method improves the LTE-RoF system without any shortcoming. Finally, at 10 dBm launch power, DMFD and EMFD methods exhibits an average signal-to-noise ratio (SNR) gain of ~ 5.95 dB and ~ 7.71 dB, respectively.

Index Terms— Long Term Evolution (LTE); Radio-over-fiber (RoF); Nonlinear Compensation; Optical OFDM (OOFDM)

I. INTRODUCTION

The actively growing end user subscriptions with bandwidth hungry, high specification, real-time, and delay-sensitive applications have been driving the mobile communications technology to continuously progress forward. The 3rd generation partnership program (3GPP) established a standard known as the LTE to support the rapidly evolving mobile communication requirements [1].

In the radio access network of LTE, eNodeB (eNB) functions as the base station (BS) similar to the global system

for mobile communications (GSM) and universal mobile telecommunication system (UMTS) BSs. However, the eNB provides the real-time operation via a 2-node architecture, without an external central controller. The 2-node architecture is achievable because the eNB architecture is designed with built-in central controller with a radio access network, and such evolution leads to costly infrastructure expansion. In addition, the vastly allocated spectrums for LTE in urban locations throughout the world are either 2.6 GHz or 1.8 GHz [2] where the drawback is the excessive loss on the wireless propagation. As a result the eNB cell radius is limited to 1 km in urban operating conditions [3]. The throughput for the user equipment (UE) at the cell edge is < 20 Mb/s from the maximum of 100 Mb/s owing to the deteriorating SNR, thus resulting in consecutive deployment of eNB at every 1 km radius in urban areas [3]. Such drastic deployment of eNB is necessary to maintain the high data throughput, which is the priority of the LTE technology.

In order to solve the problem of limited eNB cell radius, we recently proposed and extended the eNB cell radius by using a simple amplifying and forwarding (AF) type relay node (RN). The cell extension with AF type RN is only achievable due to the adoption of the RoF technology as the interface between eNB and RN [4-7]. In other word, instead of eNB, RN delivers LTE signal to UE at the cell edge. We performed a thorough LTE-RoF system integration both theoretically [4] and experimentally [5, 7] for single antenna systems. For multiple-input and multiple-output (MIMO) applications, both theoretical and experimental LTE-RoF system design was demonstrated in [6]. A new propagation region known as the optimum optical launch power region was introduced in our previous work, which exhibited a minimum system penalty within the optical launch power range of ~ -3 to ~ 2 dBm. The distortion experienced by the LTE-RoF system that degrades the quality of service (QoS) for optical launch power of < -3 dBm is linear in nature. For optical launch power of > 2 dBm, the nonlinear distortions are more detrimental compared to linear impairments. The distortions that occur below optical launch power of -3 dBm could easily be mitigated by utilizing an optical amplifier. But, such a solution is not applicable for optical launch power of > 2 dBm, due to its inherent nonlinear characteristics.

Compensating the nonlinear distortion provides an additional optical launch power gain that can minimize the power splitting losses between a single eNB and multiple RNs,

Manuscript received April 29, 2013. Thavamaran Kanesan is with Telekom Malaysia R&D, Cyberjaya, Selangor, Malaysia. (e-mail: thavamaran.kanesan@ieee.org)

Wai Pang Ng and Zabih Ghassemlooy are with the Optical Communications Research Group, Northumbria Communications Research Laboratory, Northumbria University, Newcastle-upon-Tyne, NE1 8ST U.K. (e-mail: {wai.pang.ng, z.ghassemlooy}@ieee.org).

Chao Lu is with the Photonics Research Center, Department of Electronics and Information Engineering, The Hong Kong Polytechnic University, Hung Hom, Kowloon, Hong Kong. (email: chao.lu@inet.polyu.edu.hk)

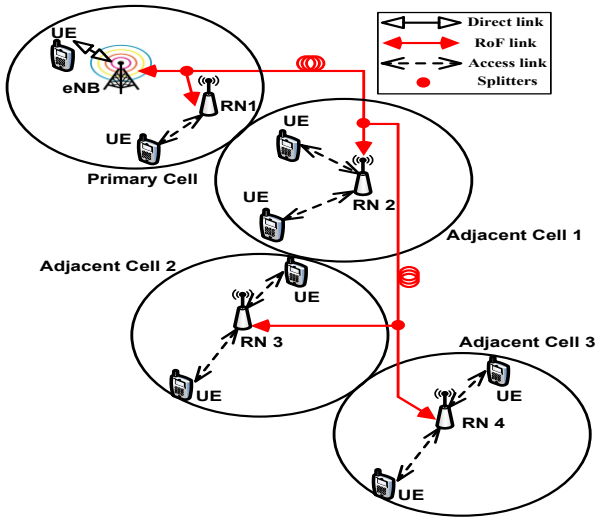


Fig. 1: Conceptual LTE-RoF network with distributed antenna network

as shown in Fig. 1. Therefore, this paper will focus on the nonlinear compensation of the LTE-RoF system to provide a higher link budget. The power gain achieved through nonlinear compensation can be used by system designers in an actual LTE RoF deployment scenario where essential splitters will be required to create a distributed antenna network. For an example, as depicted in Fig. 1, assuming a RoF system operating at the optical launch power of 10 dBm could closely achieve the performance of a RoF system operating at optimum optical launch power (~ 3 to ~ 2 dBm), then there will be about 8 - 13 dB gain. Since each splitter will introduce a 3 dB loss, then the 10 dBm optical launch power could account for 3 splitters: the 1st splitter is from the eNB of primary cell for RN1 and RN2 resulting in optical launch power of ~ 7 dBm; the 2nd splitter is in the adjacent cell 1 for RN2 and RN3 resulting in optical launch power of ~ 4 dBm; and finally the 3rd splitter scenario in the adjacent cell 2 for RN3 and RN4 that results in optical launch power of ~ 1 dBm. It is important to understand that the calculation did not take into account the optical fiber loss and the insertion loss of all three splitters. This is because the entire network design is not within the scope of this paper, but the focus is to achieve higher optical launch power levels with an optimized nonlinear compensated LTE RoF link.

In the optical fiber propagation theory, the widely known nonlinearities are the Kerr effects of self phase modulation (SPM), cross phase modulation (XPM), and four wave mixing (FWM), and the scattering phenomena of SBS and the stimulated Raman scattering (SRS). In this paper, the LTE-RoF system utilizes a single wavelength in the C-band, which is transmitted through a single mode fiber (SMF); therefore XPM, FWM and SRS are clearly negligible [8, 9]. Hence, the proposed system is only affected by SPM and SBS. In order to provide a higher link budget, higher optical launch power is required, where SBS induced nonlinear distortion has a critical effect on the system performance due to high back-reflecting power [10].

There are few methods introduced on compensating the SBS effect. Morant *et al* [11] introduced a spectrum management method for RoF system, which is only effective

for up to 15 km of SMF. A co-propagating optical signal was introduced by Downie *et al* [10] to emulate XPM in the wavelength division multiplexing (WDM) system as a compensating agent for SBS. Since our proposed system is composed of a single wavelength, the XPM based method by Downie *et al* [10] would not be applicable. Sisto *et al* [12] introduced an optimization method for biasing the modulator in order to control optical launch power, which in turn reduces the SBS effect. However, the biasing optimization adds on to the system complexity and to the inherent system noise floor due to optical amplification. Apart from optical launch power, SBS also depends on the optical fiber effective area. Sauer *et al* [13] utilized an enhanced SBS threshold optical fiber, which is designed with a bigger effective area to compensate for SBS. Enhanced SBS threshold optical fiber is not applicable for our system, because the whole idea of the proposed LTE-RoF integration is based on the existing legacy of SMF backhaul to maintain a lower deployment cost [5].

A. Proposed Solution

Taking into account of single wavelength based operation with reduced system complexity with SMF, we proposed both DMFD and EMFD methods to mitigate SBS effect in a RoF system [14]. The proposed method effectively compensates for SBS by introducing intentional laser linewidth broadening, which stops the formation of grating induced by acoustic phonons, thus reducing the back-reflected power. The SBS compensation with frequency dithering, utilizing a phase modulator, was demonstrated in [9, 15] for the cable television (CATV) technology. In this scheme the dithering frequency f_d must be twice the highest signal frequency f_m , $\{f_d > 2f_m\}$. In the case of laser based dithering, f_d was smaller than the carrier frequency for both CATV [16] and RoF applications [14]. However, no optimization was carried out to determine f_d and power limitations for laser based dithering. Since the frequency dithering method operates solely based on frequency chirping, the investigation on the effectiveness of the proposed method with two different optical modulators is crucial as DM induces an additional frequency chirp that further deteriorates the system performance, and contrariwise for EM.

In this paper we will extend on the comprehensively presented findings of [14], which shows the possibility of adopting laser based frequency dithering technique in RoF. Here we extend the work by optimizing f_d and power of the dithering signal relative to the LTE RoF system to provide an explicit guideline for system designers. In addition, this paper will provide a complete solution of DFMD and EMFD methods for LTE-RoF system, by including the analysis of quadrature phase shift keying (QPSK), 16-quadrature amplitude modulation (QAM), and 64-QAM schemes. The complete solution will also determine if an intentional additional frequency chirp via dithering will further deteriorate DM system, and the actual impact of utilizing DMFD method over EMFD method. The rest of the paper is organized as follows. Section II explains the experimental system and the theoretical background. Section III presents and discusses the obtained results. Finally, Section IV concludes the findings of the paper.

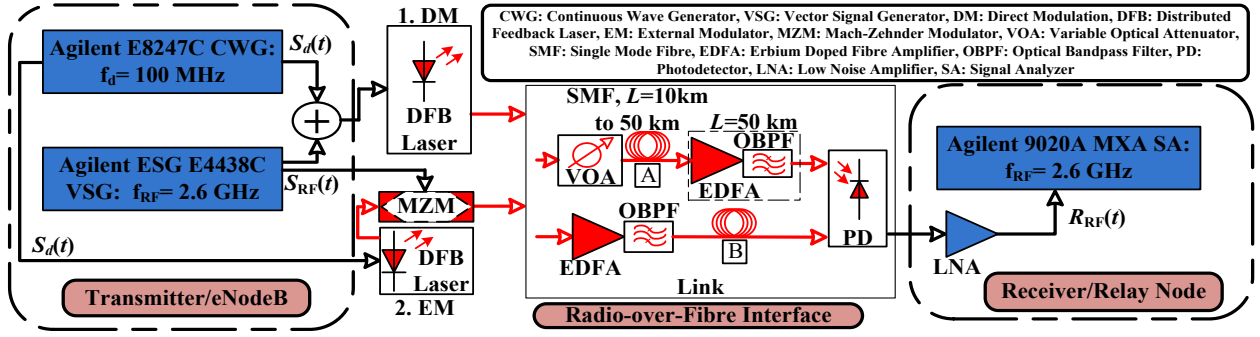


Fig. 2: The DMFD and EMFD system architecture for SBS mitigation in LTE-RoF link.

II. FUNDAMENTALS OF THE EXPERIMENTAL SYSTEM

Fig. 2 depicts the DMFD and EMFD system architecture for SBS mitigation in LTE-RoF system, and the relevant system parameters are presented in Table I. The background principals of the proposed system are as follows:

A. LTE Baseband and Passband

The LTE signal generation is performed via a vector signal generator (VSG). In the baseband, the single carrier modulations (SCMs) are composed of QPSK, 16-QAM and 64-QAM schemes. The baseband signal can be expressed as $\{X(m) : m = 0, 1, \dots, N-1\}$, where m is the subcarrier index and N is the number of subcarriers. $X(m)$ are then modulated onto orthogonal frequency division multiplexing (OFDM) $S(n)$ given by [17]:

$$S(n) = \frac{1}{\sqrt{N}} \sum_{m=0}^{N-1} X(m) e^{j2\pi mn/N}, \quad (1)$$

where $n = 0, 1, \dots, N-1$ is the time domain index. The up conversion of $S(n)$ after a digital-to-analog converter can be described as:

$$\mathcal{S}_{RF}(t) = \text{Re}\{\mathcal{S}(t) * \cos(\omega_{RF}(t))\} + \text{Im}\{\mathcal{S}(t) * \sin(\omega_{RF}(t))\}, \quad (2)$$

$$\omega_{RF} = 2\pi f_{RF}, \quad (3)$$

where $\mathcal{S}_{RF}(t)$ is the passband radio frequency (RF) OFDM signal generated at f_{RF} of 2.6 GHz and 2 dBm transmit power.

B. DMFD Signal

Two types of optical modulators are used in this paper, first is the DM via distributed feedback laser (DFB), and second is the EM via Mach-Zehnder modulator (MZM) with a DFB laser acting as the optical carrier source. The DFB laser source utilized for both DM and for EM are intentionally dithered or frequency chirped with a DMFD and EMFD signal $S_d(t)$, respectively, to broaden the linewidth of the laser. It is important to state that applying $S_d(t)$ directly to MZM will not dither the optical carrier as EM is not effected by frequency chirp. The DFB laser experience frequency dithering when $f_d \ll f_{RF}$ for RoF applications.

If $\{f_d > f_{RF}\}$, then f_d will not generate the dithering phenomenon due to the existing 2nd order harmonics in that frequency region. In other word, the DFB laser have already experienced frequency chirping from the modulation of $\mathcal{S}_{RF}(t)$ and its 2nd order harmonics, where in this case it is within the vicinity of 2.6 GHz and 5.2 GHz, respectively. Therefore, if f_d is above f_{RF} , it does not induce any additional chirping.

TABLE I: SYSTEM PARAMETERS

Parameters	Values
Dithering frequency (MHz)	100
SCM modulations	QPSK, 16-QAM, 64-QAM
Bit rate (Mb/s)	33, 66, 100
Baseband multiplexing	OFDM
Signal bandwidth (MHz)	20
Carrier frequency (GHz)	2.6
DFB bias current (mA)	60
Optical launch power (dBm)	-8 to 10
Linewidth (MHz)	11
RIN (dB/Hz)	-149.6
SMF length (km)	10 - 50
EDFA- gain, NF (dB)	4, 3.5
OBPF bandwidth (nm)	2
PD responsivity	0.42
LNA- gain, NF (dB)	18, 2.5

However, f_d does not display similar characteristic for the baseband system, because the baseband signal itself will be centered or close to the direct current. In this paper, the $S_d(t)$ signal generated via the continuous wave generator (CWG), will be optimized and analyzed conforming to the condition of $\{f_d \ll f_{RF}\}$. $\mathcal{S}_{RF}(t)$ is then combined with $S_d(t)$ prior to DM and EM.

C. Direct Modulation

The first optical modulation method is DM with the injection current $I_d(t) = \mathcal{S}_{RF}(t) + S_d(t)$. The principal of DM by adopting the intensity modulation can be expressed using the laser rate equation shown in [18]. Since frequency chirping is an integral part of frequency dithering, equation 4 describes the chirp phenomenon [4]:

$$Z(t) = e^{-\frac{1}{\tau_c}(t_{lim}-t_0)} Z(t_0) + \int_{t_0}^{t_{lim}} e^{-\frac{1}{\tau_c}(t_{lim}-t)} \frac{\Gamma}{eV} I_d(t) dt, \quad (4)$$

where $Z(t)$ is the instantaneous process of electron hole recombination with respect to Γ mode confinement factor, τ_c is the carrier decay rate, t_0 is the beginning of a symbol period, t_{lim} is the symbol period and t is the continuously varying time of the input signal, e is the electronic charge, and V is the volume. The first term of (4) is the initial condition and the second term presents the actual integral of the input signal that is bounded within the mode confinement factor. Since an integral function of a sinusoidal signal is a cosinusoidal signal as a result of phase variation. Therefore, the integral of $I_d(t)$

results in the signal phase and envelope variations, which directly represents the refractive index change of DFB and deduce the characteristic of frequency chirp.

In DM we use a DFB laser at the operating wavelength of 1551.11 nm, biased at 60 mA and injecting $S_{RF}(t)$ at 2 dBm for optimum performance [7].

D. External Modulation

The second optical modulation method adopted in this paper is MZM based EM with the operation described as follows [19]:

$$E_o(t) = E_i \cos \left[\frac{\pi (\{S_{RF}(t) + S_d\} + V_{bias})}{2 V_\pi} \right] e^{-j \left[\frac{\pi (\{S_{RF}(t) + S_d\} + V_{bias})}{2 V_\pi} \right]}, \quad (5)$$

where $E_o(t)$ and E_i are the output and input optical fields of the MZM, respectively, V_{bias} is the MZM biasing voltage, and V_π is the half-wave voltage. An Avanex X-cut single drive MZM was utilized in the experimental work, which was biased at the quadrature point. The $S_{RF}(t)$ power was maintained at 2 dBm level for consistency.

E. Principal of Laser Dithering

The intentional dithering of the DFB laser for both DM and EM for linewidth broadening can be described from the Van-der-Pol model of laser noise [20]:

$$\begin{aligned} \Delta\phi(t)^2 &= \frac{\zeta(1+\alpha^2)(t)}{2n\tau_p} \\ &= \frac{2(t)}{\tau_{coh}}, \end{aligned} \quad (6)$$

where α is the linewidth enhancement factor, n is the number of photons in the laser resonator and τ_{coh} is the coherence time of the laser, which is related to the full-width half-maximum (FWHM) of the DFB laser linewidth by:

$$\Delta\nu_{FWHM} = \frac{2}{\tau_{coh}}, \quad (7)$$

The effect $S_d(t)$ is approximately equivalent of producing multiple random spontaneous emission events, which leads to a Wiener process to the phase of the DFB laser [21]:

$$\Delta S_d(t)^2 = \frac{2(t)}{\tau_{coh d}}, \quad (8)$$

where $\tau_{coh d}$ is the coherence time of $S_d(t)$. The original coherence time of the DFB laser is τ_{coh} , but by applying the random phase modulation with $S_d(t)$, the new reduced effective coherence time of the laser at the FWHM is:

$$\frac{1}{T_{coh}} = \frac{1}{\tau_{coh}} + \frac{1}{\tau_{coh d}}, \quad (9)$$

where the reduced coherence time is equivalent to a broaden linewidth. From (8), it is clear that the optical signal propagates along SMF with a broader linewidth and is capable of blocking the formation of SBS grating, thus resulting in the reduced back-reflected power.

In order to investigate the impact of DMFD and EMFD methods in the linear region, and nonlinear regions [5], the optical launch power is varied between -8 to 10 dBm. The lower values of optical launch power are achieved via Link A

of Fig. 2, which consists of a variable optical attenuator. The erbium doped fiber amplifier (EDFA) and the optical bandpass filter (OBPF) in the Link A are only utilized for the link span of ≥ 50 km to compensate for the SMF loss as the photodetector responsivity is low. The Link B is utilized for higher values of optical launch power analysis and achieved via the aid of EDFA.

F. SMF

The transmission medium in this paper is based on SMF in the range of 10, 35, and 50 km. The nonlinear Schrodinger model that governs both the linear and nonlinear propagation can be adopted from [5]. At the receiver direct detection (DD) scheme using the Newport D8-ir photodetector is adopted. Following photodetection, the received RF LTE signal R_{RF} is amplified via a low noise amplifier and demodulated via the signal analyzer (SA).

III. RESULTS AND DISCUSSION

A. Optimization of Dithering Signal

In order to further investigate the dithering signal, an optimization of the dithering signal frequency and power will be carried out, and the outcome will be observed via the relative impact on the LTE-RoF signal transmitted at 2.6 GHz. Fig. 3 presents the optimization of the dithering signal at optical launch power of 10 dBm with a transmission span of 10 km, and the corresponding error vector magnitude (EVM) response for the LTE signal. We aim to achieve an EVM of 8% in the system design according to 3GPP LTE requirement [22]. The x-axis of Fig. 3 is the varying frequency of the dithering signal with RF power in the y-axis, and the response of the variation is shown in z-axis as the LTE signal EVM.

In Fig. 3, launching the dithering signal between 100 kHz and 14 MHz significantly increases the EVM rate. At 0 dBm the RF power and 100 kHz dithering signal frequency increases the EVM rate to $\sim 4.98\%$, while increasing the power to 10 dBm resulted in EVM of $\sim 49.4\%$. The result from [14] indicates that the uncompensated EVM at optical launch power of 10 dBm was $> 6\%$, which also will be shown in Section III. C. Transmitting the dithering signal at 100 kHz does compensate the SBS, but not effectively. This is because, the intermodulation (IMD) product arising from the mixing of dithering signal at 100 kHz and LTE signal at 2.6 GHz falls within the 20 MHz bandwidth of LTE signal. The higher RF power of 10 dBm for the dithering signal further distorts the LTE signal due to the increasing power level of the IMD product.

It is clear that as the dithering signal frequency increases, the EVM decreases until the transition at 15 MHz, where the EVM completely drops to $\sim 1.48\%$ at 0 dBm RF power. The mixing between dithering and LTE signals at 15 MHz and 2.6 GHz, respectively, resulted in the IMD product at 2.585 GHz, which is the explicit out-of-band IMD re-growth point. From dithering signal frequency of 15 MHz to 2.5 GHz, the observed EVM is as low as $\sim 1.48\%$ at 0 dBm of RF power, and can be further improved to $\sim 1.35\%$ by increasing the RF power to 10 dBm. Higher dithering signal power has the potential of increasing the laser linewidth, as more peaks will

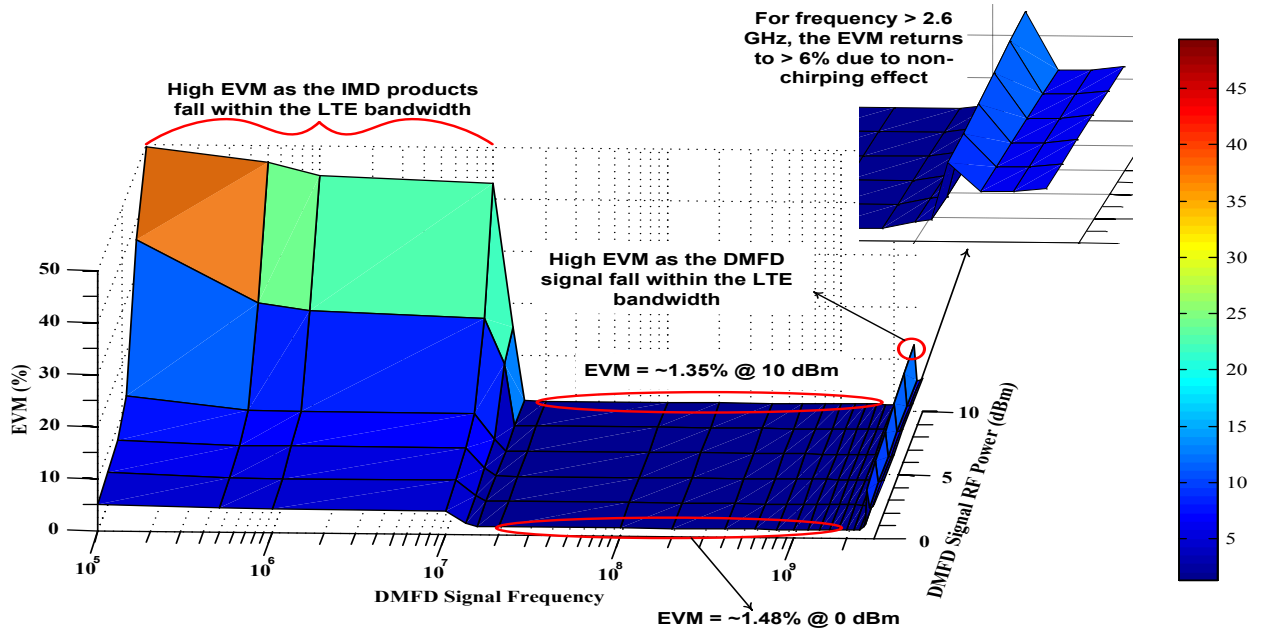


Fig. 3: Optimization of DMFD signal frequency and RF power, and its relative impact on the EVM of LTE-RoF signal

cross the FWHM limit. It is shown that further broadening of the linewidth offers higher potential for SBS compensation, however the improvement is insignificant. In line with DFB laser manufacturer recommendation of driving with 62 dBmV of average RF signal for only 60 seconds, the dithering signal power level was not increased beyond 10 dBm to ensure that the laser is not damaged.

For dithering signal above 2.5 GHz, the effect of SBS compensation reduces as the frequency chirping has already occurred in that frequency range by modulating the LTE signal. A sharp peak can be observed when the dithering signal reaches 2.6 GHz, which is due to the modulation within the bandwidth of LTE signal. Launching the dithering signal above 2.6 GHz resulted in an average EVM of ~6.45%, which achieved a close proximity with the uncompensated EVM of ~6.57%. The overall optimization of dithering method has shown that the frequency should not be lower and higher than 15 MHz and 2.5 GHz, respectively hence the expression of $\{f_d \ll f_{RF}\}$ can be rewritten as $\{f_L < f_d < f_{RF}\}$, where f_L represents the dithering boundary limit of 14 MHz.

B. SNR Penalty Analysis

We have shown that the condition of the dithering signal has changed to $\{f_L < f_d < f_{RF}\}$. Since the frequency dithering method operates based on frequency chirping, the investigation on the effectiveness of this method with two different optical modulators is crucial as DM induces PFC and contrariwise for EMs. Figs. 4(a), (b), and (c) depict the optical launch power against the SNR penalty for QPSK, 16-QAM, and 64-QAM systems, respectively, modulated onto DMFD and EMFD topologies, and transmitted over 10, 35, and 50 km SMF spans.

There are three major distinctive regions, see Fig. 4, namely; (I) linear region- PFC and chromatic dispersion (CD) induced distortions, (II) intermixing region- reduced distortion achieved by interaction between CD and PFC with SPM and SBS, and finally (III) nonlinear region- nonlinearity based

distortion from SPM and SBS effects. Regions I and II are PFC dependents. Although frequency dithering method induces frequency chirp, both DMFD and EMFD systems demonstrate resilience towards the intentional frequency chirp, thus the LTE-RoF response for regions I and II are more or less unchanged. The intentional linewidth broadening of DFB laser resulted in a linewidth of ~37.47 MHz [14], which indicates a smaller linewidth compared to conventional Fabry-Perot laser that exhibits a linewidth in the range of ~150 MHz [23], hence the invariable characteristic in regions I and II.

Since it is clear from Fig. 4 that both DMFD and EMFD methods are only effective for the region III.B and therefore the SBS threshold for the proposed system is ~6 dBm. The region III.A does not exhibit any changes from the intentional linewidth broadening for both optical modulators due to the domination of SPM. In other word, between ~2 dBm and ~6 dBm, the nonlinear distortion is in the form of amplitude to phase coupling, with no involvement of scattering or back-reflecting power.

The discussion on Fig. 4 is focused on optical launch power levels of 8 dBm and 10 dBm within the region III.B due to the effectiveness of the proposed method in this range. Only 10 and 50 km transmission spans are contemplated as the best and worst case scenarios, respectively. Overall, the system with DM demonstrated an average of ~3 dB additional penalty compared to EM for LTE RoF system due to the PFC. At optical launch power of 8 dBm in Figs. 4 (a), (b), and (c) for QPSK, 16-QAM and 64-QAM, the DMFD system SNR improvements observed for the 10 km span is ~2.33 dB, ~2.25 dB and ~2.5 dB, respectively, while the EMFD method achieved improvements of ~1.84 dB, ~2.1 dB, ~2.68 dB, respectively, for the same transmission span. The SNR gains are a measurement of the differences between uncompensated and compensated SBS link, as indicated in the region III.B of Fig. 4. For the case of 50 km transmission span at the aforementioned optical launch power, QPSK, 16-QAM, and 64-QAM exhibit SNR improvements of ~5.04 dB, ~4.39 dB

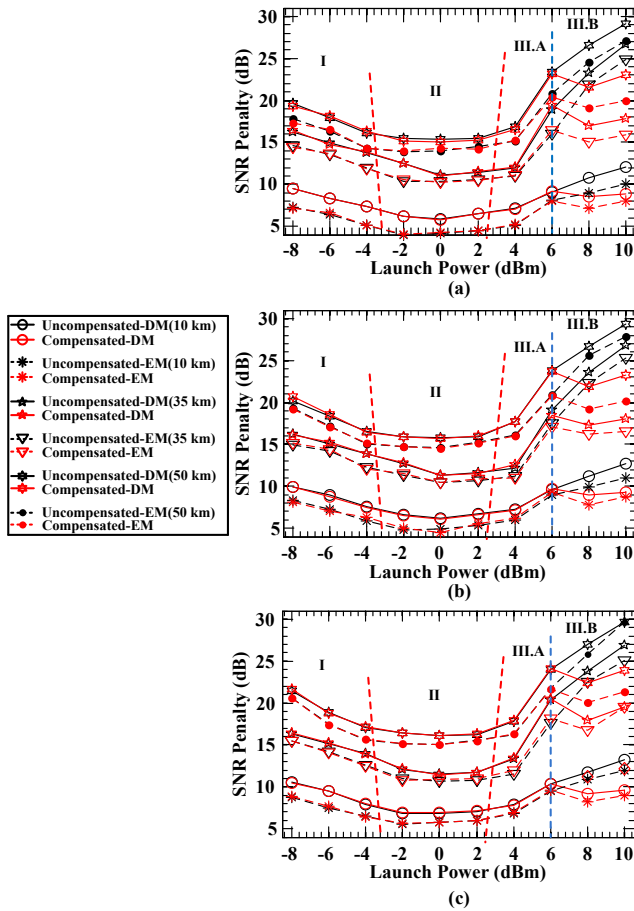


Fig. 4: Optical launch power against SNR penalty analysis for SBS compensation in (a) QPSK, (b) 16-QAM, and (c) 64-QAM with DMFD and EMFD methods over 10 km to 50 km transmission spans

and ~ 4.59 dB, respectively for the DMFD method, while the EMFD method resulted in SNR improvements of ~ 5.45 dB, ~ 6.16 dB, and ~ 5.69 dB, respectively. In the case of optical launch power of 10 dBm and 10 km transmission span, the DMFD method with QPSK, 16-QAM and 64-QAM achieved SNR gains of ~ 3.2 dB, ~ 3.31 dB, and ~ 3.55 dB, respectively, while the SNR improvements for the EMFD method is ~ 1.95 dB, ~ 2.3 dB, and ~ 3 dB, respectively. For 50 km transmission span, dithering at optical launch power of 10 dBm improved the SNR of the DMFD method by ~ 6.04 dB, ~ 6.02 dB, and ~ 5.79 dB for QPSK, 16-QAM, and 64-QAM, respectively, while the EMFD method experienced SNR gains of ~ 7.14 dB, ~ 7.62 dB, and ~ 8.37 dB, respectively.

The improvement pattern for both DMFD and EMFD methods shows that the deterioration induced by SBS is critical as the transmission span increases. Both system architectures are limited to the transmission span of 50 km, as the proposed method unable to compensate the LTE signal and achieve EVM below 8% for the transmission span above 50 km, which will be discussed in the following section with reference to Fig. 5.

C. EVM Analysis

Since the SNR penalty analysis only unfolds the system deterioration or improvement in the perspective of out-of-band distortion, then to understand the explicit system impact at the

baseband level, it is very important to utilize EVM to measure the explicit in-band distortion. Figs. 5(a), (b), and (c) depict the EVM metric of QPSK, 16-QAM, and 64-QAM systems, respectively, where the aim is to achieve lower than the 8% limit set by 3GPP. The response of regions I, II and III in Fig. 5 corresponds to the same characteristics introduced in Fig. 4. Regions I and II also shows that it is not affected by the intentional frequency chirping introduced by frequency dithering, which agrees well with results shown in Fig. 4.

The measured data for the highest optical launch power of 10 dBm, of DMFD and EMFD topologies are given in Table II. Concentrating in the region III.B, at optical launch power of 8 dBm, EMFD topology enables the LTE RoF system to achieve EVM below 8% for QPSK, 16-QAM and 64-QAM. However, the 64-QAM LTE RoF system with the DMFD topology resulted in an EVM of $\sim 8.2\%$, which is higher than the 8% limit. At 10 dBm optical launch power, both DMFD and EMFD topologies exceeded the LTE EVM limit. Although the EMFD system is superior to the DMFD system by an average of ~ 3 dB SNR gain, EVM differences are comparatively small showing the effectiveness of the DMFD system with reduced system complexity for LTE RoF applications.

Considering the highest data rate (64-QAM) and the highest transmission span (50 km), dithering for DM improved the EVM from $\sim 12.88\%$ to $\sim 8.2\%$ and EM from $\sim 12.67\%$ to $\sim 7.89\%$ for 8 dBm, while 10 dBm attained an EVM improvement of $\sim 15.02\%$ to $\sim 8.81\%$ for DM and $\sim 14.89\%$ to $\sim 8.51\%$ for EM. Now, with the optimized nonlinear

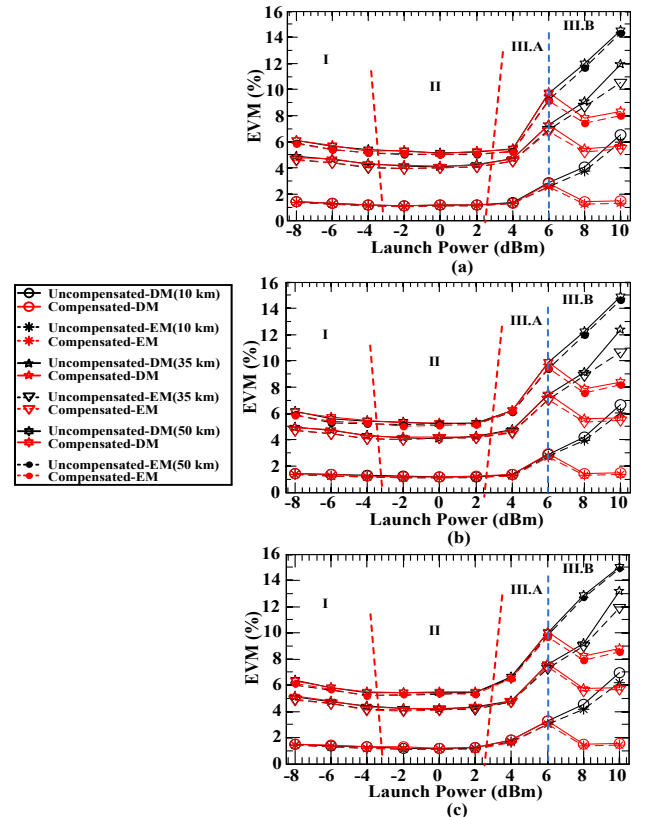


Fig. 5: Optical launch power against EVM for SBS compensation in (a) QPSK, (b) 16-QAM, and (c) 64-QAM with DMFD and EMFD methods over 10 km to 50 km transmission spans.

compensator, we are able to achieve EVM rates for higher optical launch power levels similar to the optimum optical launch power (~ 3 to ~ 2 dBm), except for longer span transmission. However, if longer transmission span is required in a network design, then forward error correction can be employed in conjunction with our proposed optimized nonlinear compensation technique.

Finally, this paper covered the nonlinear optimization of downlink transmission. The uplink system performance will be similar with our proposed nonlinear optimized link, because [24] demonstrated a full duplex LTE RoF system at low optical launch power, where with a unified transmission system, both downlink and uplink performs the same.

IV. CONCLUSION

In this paper, we have proposed and demonstrated the nonlinear compensation of LTE-RoF system based on DMFD and EMFD methods. A thorough optimization was carried out for the dithering signal, the investigation revealed that the condition of the dithering signal should meet the requirement of $\{f_L < f_d < f_{RF}\}$. It was also found that increasing the power of the dithering signal will increase the effectiveness of SBS compensation proportionally; however the EVM improvement was insignificant. The analysis between DMFD and EMFD methods showed that EM exhibited a ~ 3 dB average SNR gain over DM, however both systems achieved close proximity in the EVM measurement.

REFERENCES

- [1] T. Banham. (2010) Mobile Communications Supplement: The LTE Supplement. *informa telecoms & media*.
- [2] Real.Wireless, "LTE and HSPA Device Availability in UK-Relevant Frequency Bands," *OFCOM*, 2012.
- [3] T. Wirth, V. Venkatkumar, T. Haustein, E. Schulz, and R. Halfmann, "LTE-Advanced Relaying for Outdoor Range Extension," in *Vehicular Technology Conference Fall (VTC 2009-Fall)*, *IEEE 70th*, 2009, pp. 1-4.
- [4] T. Kanesan, W. P. Ng, Z. Ghassemlooy, and J. Perez, "Optimization of Optical Modulator for LTE RoF in Nonlinear Fiber Propagation," *Photonics Technology Letters, IEEE* vol. 24, pp. 617-619, 2012.
- [5] W. P. Ng, T. Kanesan, Z. Ghassemlooy, and C. Lu, "Theoretical and Experimental Optimum System Design for LTE-RoF Over Varying Transmission Span and Identification of System Nonlinear Limit," *Photonics Journal, IEEE*, vol. 4, pp. 1560-1571, 2012.
- [6] T. Kanesan, W. P. Ng, Z. Ghassemlooy, and C. Lu, "Theoretical and Experimental Design of an Alternative System to 2x2 MIMO for LTE over 60 km Directly Modulated RoF Link," in *Global Telecommunications Conference (GLOBECOM 2012)*, *IEEE*, Anaheim, California, pp. 1-4, 03-07 Dec 2012.
- [7] T. Kanesan, W. P. Ng, Z. Ghassemlooy, and C. Lu, "Experimental Verification of Optimized LTE-RoF System for eNB Cell Radius Improvement," *Photonics Technology Letters, IEEE*, vol. 24, pp. 2210-2213, 2012.
- [8] F. S. Yang, M. E. Marhic, and L. G. Kazovsky, "Nonlinear crosstalk and two countermeasures in SCM-WDM optical communication systems," *Lightwave Technology, Journal of*, vol. 18, pp. 512-520, 2000.
- [9] M. Jaworski and M. Marciniak, "Counteracting of stimulated Brillouin scattering in externally modulated lightwave AM-CATV systems," in *Laser and Fiber-Optical Networks Modeling, 2000. Proceedings of LFN 2000. 2nd International Workshop on*, 2000, pp. 71-73.
- [10] J. D. Downie and J. Hurley, "Experimental study of SBS mitigation and transmission improvement from cross-phase modulation in 10.7 Gb/s unrepeaters systems," *Opt. Express*, vol. 15, pp. 9527-9534, 2007.
- [11] M. Morant, T. Quinlan, S. Walker, and R. Llorente, "Complete mitigation of brillouin scattering effects in reflective passive optical

Table II: DMFD and EMFD EVM at 10 dBm optical launch powers

Launch power	Modulation schemes	Uncompensated	Compensated	Gain
10 dBm	DMFD:	10 km: $\sim 6.57\%$	$\sim 1.46\%$	$\sim 5.11\%$
	QPSK	50 km: $\sim 14.53\%$	$\sim 8.33\%$	$\sim 6.2\%$
	EMFD:	10 km: $\sim 5.95\%$	$\sim 1.31\%$	$\sim 4.64\%$
	QPSK	50 km: $\sim 14.33\%$	$\sim 8.02\%$	$\sim 6\%$
	DMFD: 16-QAM	10 km: $\sim 6.65\%$	$\sim 1.49\%$	$\sim 5.16\%$
		50 km: $\sim 14.87\%$	$\sim 8.41\%$	$\sim 6.46\%$
	EMFD: 16-QAM	10 km: $\sim 6.02\%$	$\sim 1.36\%$	$\sim 4.66\%$
		50 km: $\sim 14.62\%$	$\sim 8.22\%$	$\sim 6.4\%$
	DMFD: 64-QAM	10 km: $\sim 6.97\%$	$\sim 1.53\%$	$\sim 5.44\%$
		50 km: $\sim 15.02\%$	$\sim 8.81\%$	$\sim 6.21\%$
	EMFD: 64-QAM	10 km: $\sim 6.16\%$	$\sim 1.41\%$	$\sim 4.75\%$
		50 km: $\sim 14.89\%$	$\sim 8.51\%$	$\sim 6.38\%$

networks using triple-format OFDM radio signals," in *Optical Fiber Communication Conference and Exposition (OFC/NFOEC), 2011 and the National Fiber Optic Engineers Conference*, 2011, pp. 1-3.

- [12] M. M. Sisto, S. LaRochelle, and L. A. Rusch, "Carrier-to-noise ratio optimization by modulator bias control in radio-over-fiber links," *Photonics Technology Letters, IEEE*, vol. 18, pp. 1840-1842, 2006.
- [13] M. Sauer, A. Kobayakov, and A. B. Ruffin, "Radio-Over-Fiber Transmission With Mitigated Stimulated Brillouin Scattering," *Photonics Technology Letters, IEEE*, vol. 19, pp. 1487-1489, 2007.
- [14] T. Kanesan, W. P. Ng, Z. Ghassemlooy, and C. Lu, "Impact of Optical Modulators in LTE RoF System with Nonlinear Compensator for Enhanced Power Budget," in *Optical Fiber Communication Conference/National Fiber Optic Engineers Conference (OFC/NFOEC) 2013*, 2013, pp. 1-3.
- [15] F. W. Willems, J. C. van der Plaats, and W. Muys, "Harmonic distortion caused by stimulated Brillouin scattering suppression in externally modulated lightwave AM-CATV systems," *Electronics Letters*, vol. 30, pp. 343-345, 1994.
- [16] F. W. Willems, W. Muys, and J. S. Leong, "Simultaneous suppression of stimulated Brillouin scattering and interferometric noise in externally modulated lightwave AM-SCM systems," *Photonics Technology Letters, IEEE*, vol. 6, pp. 1476-1478, 1994.
- [17] 3GPP, "Evolved Universal Terrestrial Radio Access (E-UTRA); Physical channels and modulation (3GPP TS 36.211 V10.4.0 Rel-10)," 2011.
- [18] X. Zheng, X. Q. Jin, R. P. Giddings, J. L. Wei, E. Hugues-Salas, Y. H. Hong, and J. M. Tang, "Negative Power Penalties of Optical OFDM Signal Transmissions in Directly Modulated DFB Laser-Based IMDD Systems Incorporating Negative Dispersion Fibers," *Photonics Journal, IEEE*, vol. 2, pp. 532-542, 2010.
- [19] L. N. Binh, *Optical Fiber Communications Systems: Theory, Practice, and Matlab Simulink Models*: Taylor & Francis, 2008.
- [20] K. Vahala and A. Yariv, "Semiclassical theory of noise in semiconductor lasers - Part I, II," *Quantum Electronics, IEEE Journal of*, vol. 19, pp. 1096-1101, 1983.
- [21] S. Karlin and H. M. Taylor, *A First Course in Stochastic Processes*, 2nd ed. New York: Academic Press, 1975.
- [22] 3GPP, "EVM for LTE Repeater (3GPP TSG-RAN4 Meeting #52, TS 36.143, Rel-8)," 2009.
- [23] P. J. Probert and J. E. Carroll, "Lumped circuit model for prediction of linewidth in Fabry Perot and DFB lasers, including external cavity devices," *Optoelectronics, IEE Proceedings J*, vol. 136, pp. 22-32, 1989.
- [24] T. Kanesan, W. P. Ng, Z. Ghassemlooy, and C. Lu, "Experimental full duplex simultaneous transmission of LTE over a DWDM directly modulated RoF system," *Optical Communications and Networking, IEEE/OSA Journal of*, vol. 6, pp. 8-17, 2014.